

Original Article

Ferroptosis was involved in the oleic acid-induced acute lung injury in mice

ZHOU Hang^{1,2}, LI Feng^{1,2}, NIU Jian-Yi^{1,2}, ZHONG Wei-Yong^{1,2}, TANG Min-Yu^{1,2}, LIN Dong^{1,2}, CUI Hong-Hui^{1,2}, HUANG Xue-Han^{1,2}, CHEN Ying-Ying^{1,3}, WANG Hong-Yan⁴, TU Yong-Sheng^{1,*}

¹Department of Physiology, School of Basic Medical Sciences; ²The First Clinical Medical College; ³The Sixth Clinical Medical College; ⁴Department of Pathology, School of Basic Medical Sciences, Guangzhou Medical University, Guangzhou 511436, China

Abstract: The aim of the present study was to investigate the role of ferroptosis in acute lung injury (ALI) mouse model induced by oleic acid (OA). ALI was induced in the mice via the lateral tail vein injection of pure OA. The histopathological score of lung, lung wet-dry weight ratio and the protein content of bronchoalveolar lavage fluid (BALF) were used as the evaluation indexes of ALI. Iron concentration, glutathione (GSH) and malondialdehyde (MDA) contents in the lung tissues were measured using corresponding assay kits. The ultrastructure of pulmonary cells was observed by transmission electron microscope (TEM), and the expression level of prostaglandin-endoperoxide synthase 2 (PTGS2) mRNA was detected by quantitative polymerase chain reaction (q-PCR). Protein expression levels of glutathione peroxidase 4 (GPX4), ferritin and transferrin receptor 1 (TfR1) in lung tissues were determined by Western blot. The results showed that histopathological scores of lung tissues, lung wet-dry weight ratio and protein in BALF in the OA group were higher than those of the control group. In the OA group, the mitochondria of pulmonary cells were shrunken, and the mitochondrial membrane was ruptured. The expression level of PTGS2 mRNA in the OA group was seven folds over that in the control group. Iron overload, GSH depletion and accumulation of MDA were observed in the OA group. Compared with the control group, the protein expression levels of GPX4 and ferritin in lung tissue were down-regulated in the OA group. These results suggest that ferroptosis plays a potential role in the pathogenesis of ALI in our mouse model, which may provide new insights for development of new drugs for ALI.

Key words: acute lung injury; oleic acid; ferroptosis; glutathione; glutathione peroxidase 4; iron

铁死亡参与油酸诱导的小鼠急性肺损伤

周航^{1,2}, 李凤^{1,2}, 牛建一^{1,2}, 钟伟勇^{1,2}, 汤敏誉^{1,2}, 林栋^{1,2}, 崔洪珩^{1,2}, 黄学涵^{1,2}, 陈莹莹^{1,3}, 王红艳⁴, 涂永生^{1,*}

广州医科大学¹基础医学院生理教研室; ²第一临床学院; ³第六临床学院; ⁴基础医学院病理教研室, 广州 511436

摘要: 本研究旨在探讨铁死亡在油酸(oleic acid, OA)致急性肺损伤(acute lung injury, ALI)小鼠模型中的作用。小鼠尾静脉注射纯OA制备ALI模型, 以肺组织病理学评分、肺湿干重比、支气管肺泡灌洗液(bronchoalveolar lavage fluid, BALF)蛋白含量作为ALI的评价指标, 用试剂盒检测肺组织的铁浓度、谷胱甘肽(glutathione, GSH)和丙二醛(malondialdehyde, MDA)含量, 用透射电子显微镜观察肺细胞的超微结构, 用定量PCR (q-PCR)检测肺组织中前列腺素内过氧化物合酶2 (prostaglandin-endoper-

Received 2019-02-28 Accepted 2019-07-01

This work was supported by the Natural Science Foundation of Guangdong Province, China (No. 2018A0303130256), the Medical Scientific Research Foundation of Guangdong Province, China (No. A2017315, A2018390 and A2019042), the Laboratory Open Project for College Students of Guangzhou Medical University, the National College Students' Innovation Entrepreneurship Training Program of China (No. 20181057000), the Guangzhou Medical University College Students Science Technology Innovation Project (No. 2017A006), Special Funds for the Cultivation of Guangdong Provincial College Students' Scientific and Technological Innovation, and "Climbing Program" Special Funds (No. pdjhb0419).

*Corresponding author. Tel: +86-20-37103213; Fax: 86-20-37103213; E-mail: tuys@gzhmu.edu.cn

oxide synthase 2, PTGS2) mRNA表达, 用Western blot测定肺组织谷胱甘肽过氧化物酶4 (glutathione peroxidase 4, GPX4)、铁蛋白和转铁蛋白受体1 (transferrin receptor 1, TfR1)的蛋白表达水平。结果表明, OA组小鼠肺组织病理评分、肺湿干重比和BALF中蛋白均高于对照组。OA组小鼠肺细胞线粒体缩小, 线粒体膜破裂。与对照组相比, OA组PTGS2 mRNA表达增加7倍。OA组小鼠肺组织出现铁过载、GSH含量减少和MDA累积。与对照组相比, OA组小鼠肺组织GPX4和铁蛋白表达水平下调。以上结果提示, 铁死亡可能在ALI发病机制中发挥作用, 这为治疗ALI的新药开发提供了新的角度。

关键词: 铁死亡; 油酸; 急性肺损伤; 谷胱甘肽; 谷胱甘肽过氧化物酶4; 铁

中图分类号: R363

Acute lung injury (ALI) characterized by uncontrolled inflammation is a main cause of death with a high mortality rate of over 30%, despite the advancements of new treatment techniques for ALI therapy^[1]. Multiple forms of cell death such as necrosis, apoptosis, autophagy and necroptosis have been studied in the lung of humans and experimental animals of ALI^[2–6]. Therefore, it is necessary to investigate the novel cellular and molecular basis of ALI.

Recently, ferroptosis, which differs from other types of cell death in mechanism and morphology, has been reported in acute and chronic diseases including brain, kidney, and liver injury/diseases except ALI^[7–12]. Ferroptosis may represent a potential therapeutic target against brain, kidney, and liver injury/diseases. The characteristic morphological features of ferroptosis include shrunken mitochondria, increased mitochondrial membrane density and membrane rupture^[8, 10]. Besides, the initiation of ferroptosis depends on three critical events, accumulation of lipid peroxidation, iron overload and glutathione (GSH) depletion^[13, 14]. Fe²⁺ reduces oxygen to form superoxide radicals which cause lipid peroxidation and subsequent damage to cells through Fenton reaction^[15, 16]. GSH can act as a reductant in the presence of GSH peroxidase (GPX) to reduce H₂O₂ or other hydroperoxides to less toxic substances^[17]. It has been previously reported that superfluous iron was observed in lower respiratory tract of ALI patients^[18, 19]. Moreover, the deficiency in total GSH and increase in oxidized GSH (GSSG) were found in the alveolar epithelial lining fluid of patients with ALI^[20–22] and animal ALI models^[23, 24]. In this context, we hypothesized that superfluous iron and GSH depletion might induce ferroptosis in lung tissues of ALI. In the present study, we established oleic acid (OA)-induced ALI mouse model and investigated lipid peroxidation, iron overload and GSH depletion in lung tissue, hoping to discover a new possible mechanism for the pathophysiology of ALI.

1 MATERIALS AND METHODS

1.1 Animal model of ALI

Mouse model of ALI was established as described in our previous studies^[3]. Male C57BL/6 mice (Southern Medical University Experimental Animal Center) weighed 18–22 g, aged 6–8 weeks. Eighteen mice were randomly assigned into control and OA groups. Mice in OA group were injected via the lateral tail vein with pure OA at a dose of 250 μL/kg, while control mice received an injection of an equal volume of normal saline (NS). At 6 h after injection of OA, the inferior lobe of right lung was excised for measurement of lung wet-dry weight ratio. Other parts of lung tissue were removed after pulmonary circulation perfusion. Then the rest of right lung was used for the hematoxylin and eosin (H&E) staining and transmission electron microscopy examination. After bronchoalveolar lavage, the left lung was used for detecting iron content, total GSH and reduced GSH assay, malondialdehyde (MDA) assay, Western blot and quantitative real time polymerase chain reaction (q-PCR). Then the bronchoalveolar lavage fluid (BALF) was immediately determined by BCA Protein Assay Kit (Beyotime Institute of Biotechnology, Shanghai, China) according to the manufacturer's instructions. All animal experiments were performed in accordance with the "Guideline for the Care and Use of Laboratory Animals" of China and approved by Animal Care and Use Committee of Guangzhou Medical University (Laboratory Animal Ethics No. GY2017-043).

1.2 Analysis of iron content in lung

Lung tissues were removed and homogenized on the ice bath for 10 min for following studies. Samples were added by steps, and heated on boiling water bath for 5 min, then cooled and centrifuged at 3 500 r/min for 10 min. The supernatant was detected at a wavelength of 520 nm. Iron concentration in the mouse lung was measured using an iron assay kit according to the manufac-

turer's protocol (Jiancheng Bioengineering Institute, China). In this method, under the action of acidic solution and reductant, iron in ferritin is separated from protein. After ferric iron is reduced to ferrous form, iron reacts with sulfadiazine and trimethoprim to form stable and colored complexes. Within a certain range, the amount of iron is proportional to the color.

1.3 Total GSH and reduced GSH assay

Lung tissues were homogenized on ice (40 mg tissue in 360 μ L PBS solution). Then the homogenates were centrifuged at 10 000 g for 10 min, and the supernatant was used for GSH and GSSG assays. Total GSH and reduced GSH levels were measured by the colorimetric microplate assay kits (Beyotime Institute of Biotechnology, Shanghai, China) according to the manufacturer's instructions. The formation of 2-nitro-5-thiobenzoic acid, which was proportional to the concentration of GSH, was analyzed directly at 412 nm using a microplate reader (Bio-Rad, California, USA). The GSSG level was quantified by the same method of total GSH assay after removing the reduced GSH. The amount of reduced GSH was obtained by subtracting the amount of GSSG from that of the total GSH.

1.4 MDA assay

Lung tissues were homogenized on ice, then the homogenates were centrifuged at 3 000 r/min for 5 min at 4 °C. The level of MDA in mouse lung tissues was analyzed by using an MDA assay kit (Jiancheng Bioengineering Institute, China). MDA reacts with thiobarbituric acid (TBA) under acidic and high temperature conditions to form a stable chromophoric production, which can be measured at a wavelength of 532 nm.

1.5 H&E staining

H&E staining was performed as previously described^[25,26]. After immersion in 4% paraformaldehyde for 24 h and then transferred to 70% ethanol, then lung tissues were stained with H&E and examined by a light microscopy. According to our previous research, we used a scoring system to evaluate the histopathological injury^[27].

1.6 Western blot

Western blot was performed as described previously^[3]. Samples collected from mouse lung tissues were lysed with cold cell lysis buffer and subjected to SDS-PAGE. Proteins were then transferred onto PVDF membranes, blocked, and then exposed to primary antibodies including anti-ferritin (1:1 000; ab75973, Abcam, Cambridge, UK), anti-transferrin receptor 1 (TfR1; 1:2 000; ab84036, Abcam, Cambridge, UK), anti-GPX4

(1:2 000; ab125066, Abcam, Cambridge, UK) and anti- β -actin (1:5 000; Cell Signaling Technology, Beverly, USA). Afterwards, the horseradish peroxidase-conjugated antibody was incubated in a 1:2 000 dilution for 1 h at room temperature. Finally, the chemiluminescence method was used to detect the protein expression.

1.7 Measurement of lung wet-dry weight ratio

Lung wet-dry weight ratio was measured as described previously^[27]. Lung tissues were removed and weighed immediately. After being washed away blood on lung surface, the lung tissues were dried in an oven at 60 °C for 72 h and reweighed. The lung wet-dry weight ratio was calculated by dividing the mass of the initial specimen by the mass of the dried specimen. The wet-dry weight ratio was used as an indicator of lung edema.

1.8 Transmission electron microscopy examination

Lung tissues were obtained immediately after anesthesia of the mice and cut into small pieces (1 mm³). The specimens were fixed with 2% glutaraldehyde at 4 °C, washed in the 0.1 mol/L phosphate buffer (pH 7.4), fixed with 1% osmium tetroxide, and stained with 1% aqueous uranyl acetate. Specimens were placed with capsules contained embedding medium and heated at 70 °C for about 48 h. The specimen sections were stained with uranyl acetate and alkaline lead citrate respectively and observed in transmission electron microscope (TEM) of Jeol JEM 1400 (Tokyo, Japan).

1.9 q-PCR

q-PCR was performed as described earlier^[28]. RNA extraction was performed by using TRIzol Reagent (Invitrogen, California, USA) in accordance with the manufacturer's instructions. Then first-strand complementary DNA was synthesized and amplified by using KAPA SYBR FAST One-Step qRT-PCR Kits (Kapa-biosystems, Cape Town, South Africa) according to the manufacturer's instructions. The following primer pairs were used: mouse prostaglandin-endoperoxide synthase 2 (PTGS2): Forward: 5'-TGGAGGCGAAGTGG-GTTTTA-3', Reverse: 5'-GAGTGGGAGGCACTTG-CATT-3'; GAPDH: Forward: 5'-GGCCTCCAAGGAG-TAAGAAA-3', Reverse 5'-GCCCTCCTGTTATTATGG-3'. The level of GAPDH mRNA expression was used as an internal control. Ultimately, the relative level of mRNA was analyzed by using the 2^{- $\Delta\Delta$ Ct} method.

1.10 Statistical analyses

The whole experiments were repeated three or more times independently. Data were expressed as mean \pm SD. Comparison of two groups were analyzed by using

the two independent sample *t*-test. *P*-values < 0.05 were considered to be statistically significant.

2 RESULTS

2.1 ALI was successfully induced by tail vein injection of OA

We combined BALF protein concentration, the lung tissue wet-dry weight ratio, and H&E staining to assess the extent of lung injury in mice after OA injection. The wet-dry weight ratio of lung tissues in the OA group was higher than the saline control group (Fig. 1A), and the BALF protein concentration in the OA group was significantly higher than that of control group (Fig. 1B). These data indicated that the water content in lung tissue of OA group was increased, presenting the increased permeability of alveoli. Then, we used H&E staining to assess the degree of lung injury (Fig. 1C). It was observed that there were evident pathological changes in the lungs of the OA group, including neutrophil infiltration and hyperemia in the alveolar and interstitial space, thickening of the alveolar wall, conspicuous pulmonary edema, and formation of

the hyaline membrane. Finally, the histopathological scores of OA group were strikingly higher, as compared with control group (Fig. 1D). Collectively, it was proved that the ALI mouse model was successfully constructed 6 h after OA injection.

2.2 Ferroptosis was found in lung tissues of ALI mouse model

Electron microscope pictures of mouse lung tissue showed that the alveolar type II epithelial cells of OA group exhibited the abnormal mitochondrial morphology typical of ferroptosis, including shrunken mitochondria (single white arrow) and mitochondrial membrane rupture (paired white arrow) (Fig. 2A). It was also observed that the expression of ferroptosis biomarkers PTGS2 mRNA in the OA group was 7-fold over that in the control group (Fig. 2B). These phenomena indicated that ferroptosis occurred in the OA-induced mouse ALI.

2.3 Impaired GSH-GPX and iron metabolism regulation system were concomitant with the occurrence of ferroptosis

Ferroptosis is triggered by lipid peroxidation in cells,

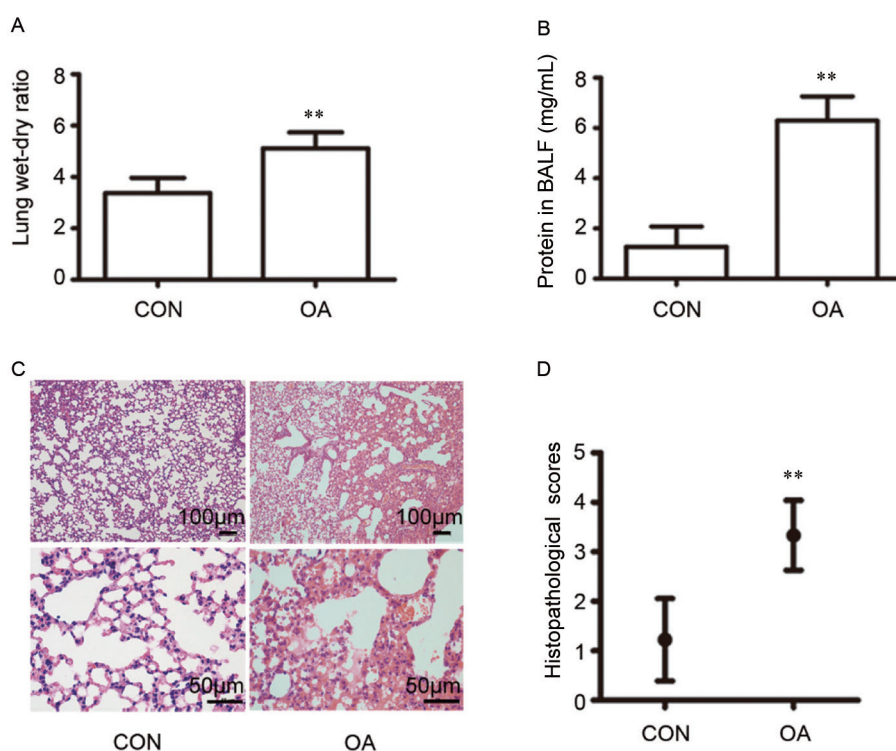


Fig. 1. Acute lung injury was successfully induced by tail vein injection of oleic acid. *A*: The wet-dry weight ratio of the lung tissue in OA and control groups. *B*: The BALF protein concentration. *C*: H&E staining of lung tissues. Scale bar, 50 μm or 100 μm. *D*: Histopathological scores. Mean ± SD. The results were repeated independently at least three times. CON: control; OA: oleic acid. ***P* < 0.01 vs control.

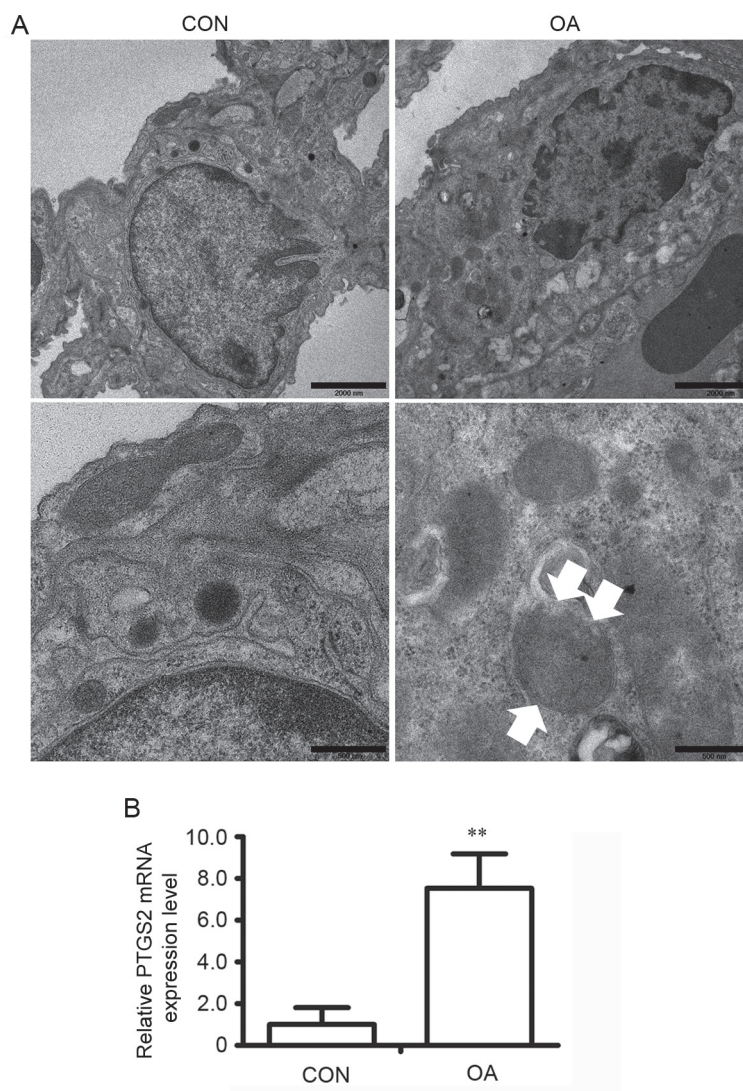


Fig. 2. Ferroptosis was found in lung tissues of ALI mouse model by transmission electron microscopy. *A*: Transmission electron microscopy results showed shrunken mitochondria (single white arrow) and mitochondrial membrane rupture (paired white arrow) in the OA group. Scale bar indicates 2 000 nm or 500 nm. *B*: The marker gene of ferroptosis, PTGS2 mRNA expression was significantly higher in ALI model than that in the control. Mean \pm SD. The q-PCR results were repeated at least three times. CON: control; OA: oleic acid. ** $P < 0.01$ vs control.

so we measured the level of MDA which is the main end product of lipid peroxidation. The MDA level of the OA group was higher than the control group (Fig. 3A). It has been known that the accumulation of lipid ROS is caused by the depletion of the intracellular antioxidant GSH. Therefore, we next measured the levels of reduced GSH and total GSH. We observed decreases in the levels of total GSH and reduced GSH in OA-induced ALI mice (Fig. 3B). Since previous studies have reported that depletion of GSH leads to inactivation of GPXs^[8], we measured the expression of GPX4. Results of Western blot showed that GPX4 protein

expression was reduced in OA-induced ALI mice (Fig. 3C, D). Taken together, these results indicated that decrease of GSH and inactivation of GPX4 might induce ferroptosis.

When iron absorption is abnormally increased, it causes excessive intracellular iron accumulation, which in turn triggers more Fenton reaction, leading to lipid peroxidation and eventual ferroptosis. Hence, we further measured the levels of TfR1, iron and ferritin. The results illustrated that the iron content in the pulmonary cells of OA group was increased (Fig. 3E). Moreover, Western blot revealed a decrease in ferritin expression

(Fig. 3F, G), but without alteration of TfR1 expression compared with control group (Fig. 3H, I). It appeared that iron uptake and metabolism in cells were closely related to the occurrence of ferroptosis.

3 DISCUSSION

Ferroptosis has been shown to occur in macrophage^[29], kidney tubule cells^[30], cancer cells^[10], neurons^[7] and T cells^[31]. However, occurrence of ferroptosis in ALI is still unexplored. In this study, we aimed to show the occurrence of ferroptosis in ALI mouse model. The present research found typical ferroptotic morphological changes, GSH depletion with downregulated GPX4, lipid peroxidation and iron accumulation in the lungs of ALI mouse model, which implicates ferroptosis might be associated with the pathogenesis of ALI.

First, ALI model was evaluated by the H&E staining,

histopathological scores of lung tissues, protein content of BALF and lung wet-dry weight ratio. The results revealed the evidence of lung injury such as accumulation of neutrophils, formation of hyaline membranes, alveolar edema and increased protein in BALF, thus confirming that OA induced ALI in mice.

Furthermore, we found ferroptosis was associated with the ALI mouse model. Ferroptosis has distinct morphological characteristics, differing from other known types of cell death^[32]. According to previous reports, ferroptosis is morphologically characterized by shrunken mitochondria^[7], mitochondrial membrane rupture, reduction of mitochondria crista, and decrease in mitochondrial size^[8, 10]. In line with these reports, shrunken mitochondria and mitochondrial membrane rupture were also observed in pulmonary cells of the OA group. Additionally, mRNA expression of PTGS2, the marker gene of ferroptosis^[33], was seven folds over

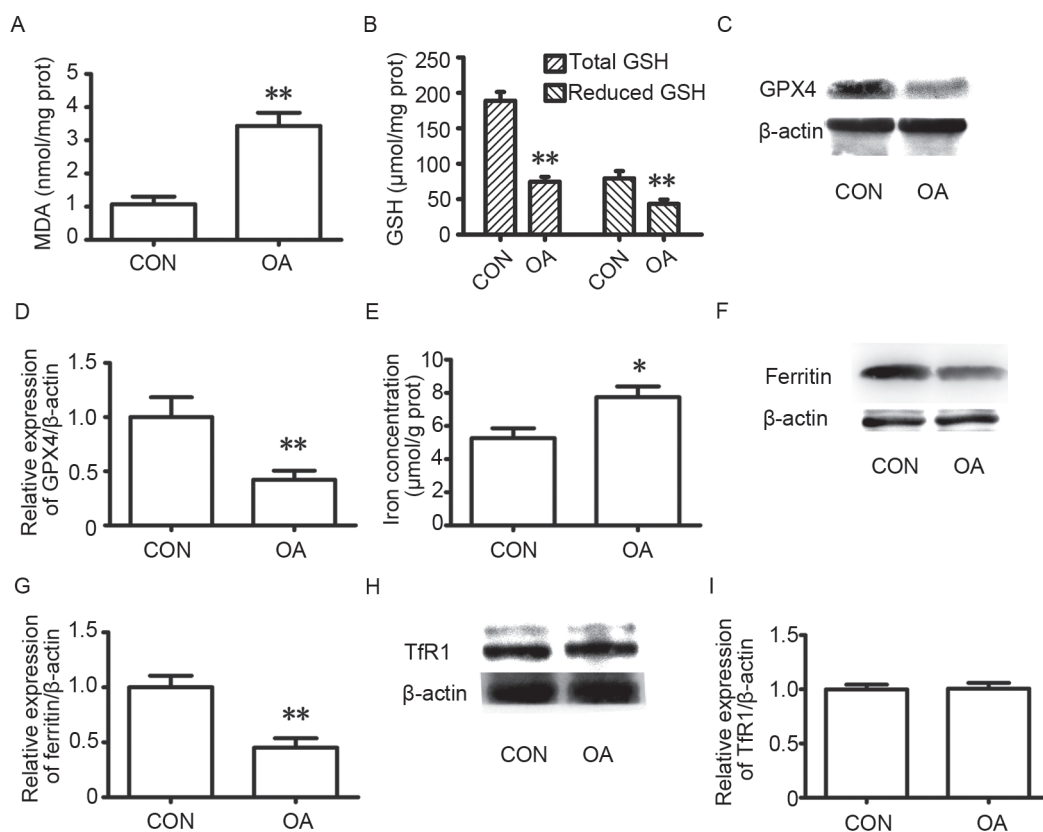


Fig. 3. Impaired GSH-GPX and iron metabolism regulation system were concomitant with the occurrence of ferroptosis. *A*: Malondialdehyde (MDA) production was elevated in lung tissues compared with that of the control group. *B*: Total GSH and reduced GSH levels were decreased in the OA group. *C, D*: Western blot results showed downregulated GPX4 in the OA group. *E*: Iron concentration was higher in the OA group. *F, G*: Western blot results showed decreased ferritin in the OA group. *H, I*: TfR1 protein expression was not altered. Mean \pm SD. The results were repeated independently at least three times. CON: control; OA: oleic acid. * $P < 0.05$, ** $P < 0.01$ vs control.

the control group. Together, it seems likely that ferroptosis occurred in ALI.

We further addressed the mechanisms of ferroptosis in ALI mouse model. Ferroptosis has been characterized by impaired GSH-GPX4 antioxidant system, iron accumulation and lipid ROS production. We first tested GSH-GPX4 regulatory system which is a crucial regulator for ferroptosis^[33]. We found that the total GSH, reduced GSH and GPX4 protein were all decreased in the OA group. It has been reported that depletion of GSH and lessening GPX4 lead to ferroptosis^[13]. And lipid peroxidation could be exacerbated when there are decreased levels of GSH and GPX4, since GSH is a scavenger of MDA upon being catalyzed by GPX4^[34]. Moreover, iron promotes the production of superoxide radicals via the Fenton reaction, which can result in lipid peroxidation^[35]. Thus we further surveyed the iron metabolism and lipid peroxidation. We found that iron concentration was significantly increased in lung tissues of the OA group, and ferritin was decreased without any changes of TfR1. In consistent with our findings, other groups also found that iron concentration was increased in lung lining fluid of patients with ALI^[36] and in lung tissues of ALI rats^[37]. A down-regulation of ferritin in the lungs of acute respiratory distress syndrome (ARDS) caused the accumulation of cellular iron due to the damage of iron storage protein^[37]. Iron, which is mainly stored in ferritin^[38], could be released by degradation of ferritin, and subsequently enormous iron would contribute to Fenton reaction, and then massive lipid peroxidation products were generated to prompt ferroptosis^[39,40]. Thus, it suggested that such a response might place pulmonary cells at risk of ferroptosis. But TfR1 in the OA group was not altered compared with the control group, thus TfR1 appeared not to be the main promoter for iron import in ALI mice. In brief, depletion of GSH, decrease of GPX4, excessive iron and accumulation of lipid peroxidation occurred in ALI model may cause ferroptosis. However, the molecular signal pathways of the lipid peroxidation engendering ferroptosis in ALI model remain to be further elucidated.

In summary, in the present research, we found that ferroptosis was involved in ALI mouse model, which enhances our understanding of the pathogenesis of ALI. Our findings provide a novel perspective for development of new drugs for ALI. Additional studies are needed to determine whether the inhibitors of ferroptosis could rescue the mice from ALI through inhibition of ferroptosis.

REFERENCES

- 1 Nanchal RS, Truweit JD. Recent advances in understanding and treating acute respiratory distress syndrome. *F1000Res* 2018; 7. pii: F1000 Faculty Rev-1322.
- 2 Matute-Bello G, Winn RK, Jonas M, Chi EY, Martin TR, Liles WC. Fas (CD95) induces alveolar epithelial cell apoptosis *in vivo* implications for acute pulmonary inflammation. *Am J Pathol* 2001; 158(1): 153–161.
- 3 Pan L, Yao DC, Yu YZ, Chen BJ, Li SJ, Hu GH, Xi C, Wang ZH, Li JH, Long J, Tu YS. Activation of necroptosis in a rat model of acute respiratory distress syndrome induced by oleic acid. *Acta Physiol Sin (生理学报)* 2016; 68(5): 661–668.
- 4 Lin L, Zhang L, Yu L, Han L, Ji W, Shen H, Hu Z. Time-dependent changes of autophagy and apoptosis in lipopoly-saccharide-induced rat acute lung injury. *Iran J Basic Med Sci* 2016; 19: 632–637.
- 5 Albertine KH, Soulier MF, Wang Z, Ishizaka A, Hashimoto S, Zimmerman GA, Matthay MA, Ware LB. Fas and fas ligand are up-regulated in pulmonary edema fluid and lung tissue of patients with acute lung injury and the acute respiratory distress syndrome. *Am J Pathol* 2002; 161: 1783–1796.
- 6 Tang PS, Mura M, Seth R, Liu M. Acute lung injury and cell death: how many ways can cells die? *Am J Physiol Lung Cell Mol Physiol* 2008; 294(4): L632–L641.
- 7 Xie BS, Wang YQ, Lin Y, Mao Q, Feng JF, Gao GY, Jiang JY. Inhibition of ferroptosis attenuates tissue damage and improves long-term outcomes after traumatic brain injury in mice. *CNS Neurosci Ther* 2018; 25(4): 1–11.
- 8 Friedmann Angeli JP, Schneider M, Proneth B, Tyurina YY, Tyurin VA, Hammond VJ, Herbach N, Aichler M, Walch A, Eggenhofer E, Basavarajappa D, Radmark O, Kobayashi S, Seibt T, Beck H, Neff F, Esposito I, Wanke R, Forster H, Yefremova O, Heinrichmeyer M, Bornkamm GW, Geissler EK, Thomas SB, Stockwell BR, O'Donnell VB, Kagan VE, Schick JA, Conrad M. Inactivation of the ferroptosis regulator Gpx4 triggers acute renal failure in mice. *Nat Cell Biol* 2014; 16(12): 1180–1191.
- 9 Wang H, An P, Xie E, Wu Q, Fang X, Gao H, Zhang Z, Li Y, Wang X, Zhang J, Li G, Yang L, Liu W, Min J, Wang F. Characterization of ferroptosis in murine models of hemochromatosis. *Hepatology* 2017; 66(2): 449–465.
- 10 Dixon SJ, Lemberg KM, Lamprecht MR, Skouta R, Zaitsev EM, Gleason CE, Patel DN, Bauer AJ, Cantley AM, Yang WS, Morrison B 3rd, Stockwell BR. Ferroptosis: an iron-dependent form of nonapoptotic cell death. *Cell* 2012; 149(5): 1060–1072.
- 11 Yu H, Guo P, Xie X, Wang Y, Chen G. Ferroptosis, a new form of cell death, and its relationships with tumourous diseases. *J Cell Mol Med* 2017; 21(4): 648–657.
- 12 Stockwell BR, Friedmann Angeli JP, Bayir H, Bush AI, Con-

- rad M, Dixon SJ, Fulda S, Gascon S, Hatzios SK, Kagan VE, Noel K, Jiang X, Linkermann A, Murphy ME, Overholtzer M, Oyagi A, Pagnussat GC, Park J, Ran Q, Rosenfeld CS, Salnikow K, Tang D, Torti FM, Torti SV, Toyokuni S, Woerpel KA, Zhang DD. Ferroptosis: a regulated cell death nexus linking metabolism, redox biology, and disease. *Cell* 2017; 171(2): 273–285.
- 13 Bertrand RL. Iron accumulation, glutathione depletion, and lipid peroxidation must occur simultaneously during ferroptosis and are mutually amplifying events. *Med Hypotheses* 2017; 101: 69–74.
- 14 Yang WS, Stockwell BR. Ferroptosis: death by lipid peroxidation. *Trends Cell Biol* 2016; 26(3): 165–176.
- 15 Scindia Ph DY, Leeds Md J, Swaminathan Md S. Iron homeostasis in healthy kidney and its role in acute kidney injury. *Semin Nephrol* 2019; 39(1): 76–84.
- 16 Crichton RR, Wilmet S, Leggsyer R, Ward RJ. Molecular and cellular mechanisms of iron homeostasis and toxicity in mammalian cells. *J Inorg Biochem* 2002; 91: 9–18.
- 17 Meister A, Anderson ME. Glutathione. *Ann Rev Biochem* 2012; 52: 711–760.
- 18 Ghio AJ, Carter JD, Richards JH, Richer LD, Grissom CK, Elstad MR. Iron and iron-related proteins in the lower respiratory tract of patients with acute respiratory distress syndrome. *Crit Care Med* 2003; 31(2): 395–400.
- 19 Stites SW, Plautz MW, Bailey K, O'Brien-Ladner AR, Weselius LJ. Increased concentrations of iron and isoferritins in the lower respiratory tract of patients with stable cystic fibrosis. *Am J Respir Crit Care Med* 1999; 160: 796–801.
- 20 Pacht ER, Timerman AP, Lykens MG, Merola J. Deficiency of alveolar fluid glutathione in patients with sepsis and the adult respiratory distress syndrome. *Chest* 1991; 100(5): 1397–1403.
- 21 Schmidt R, Luboinski T, Markart P, Ruppert C, Daum C, Grimminger F, Seeger W, Gunther A. Alveolar antioxidant status in patients with acute respiratory distress syndrome. *Eur Respir J* 2004; 24(6): 994–999.
- 22 Bunnell E, Pacht ER. Oxidized glutathione is increased in the alveolar fluid of patients with the adult respiratory distress syndrome. *Am Rev Respir Dis* 1993; 148: 1174–1178.
- 23 Laurent T, Markert M, Feihl F, Schaller MD, Perret C. Oxidant-antioxidant balance in granulocytes during ARDS. Effect of N-acetylcysteine. *Chest* 1996; 109(1): 163–166.
- 24 Britt RD Jr, Velten M, Locy ML, Rogers LK, Tipple TE. The thioredoxin reductase-1 inhibitor aurothioglucose attenuates lung injury and improves survival in a murine model of acute respiratory distress syndrome. *Antioxid Redox Signal* 2014; 20(17): 2681–2691.
- 25 Tang FC, Wang HY, Ma MM, Guan TW, Pan L, Yao DC, Chen YL, Li SJ, Yang H, Zhu XQ, Tu YS. Simvastatin attenuated rat thoracic aorta remodeling by decreasing ROCK2-mediated CyPA secretion and CD147-ERK1/2-cyclin pathway. *Mol Med Rep* 2017; 16(6): 8123–8129.
- 26 Tang FC, Wang HY, Ma MM, Guan TW, Pan L, Yao DC, Chen YL, Chen WB, Tu YS, Fu XD. CyPA-CD147-ERK1/2-cyclin D2 signaling pathway is upregulated during rat left ventricular hypertrophy. *Acta Physiol Sin (生理学报)* 2015; 67(5): 393–400.
- 27 Pan L, Yao DC, Yu YZ, Li SJ, Chen BJ, Hu GH, Xi C, Wang ZH, Wang HY, Li JH, Tu YS. Necrostatin-1 protects against oleic acid-induced acute respiratory distress syndrome in rats. *Biochem Biophys Res Commun* 2016; 478(4): 1602–1608.
- 28 Tu YS, He J, Liu H, Lee HC, Wang H, Ishizawa J, Allen JE, Andreeff M, Orlowski RZ, Davis RE, Yang J. The imipridone ONC201 induces apoptosis and overcomes chemotherapy resistance by up-regulation of bim in multiple myeloma. *Neoplasia* 2017; 19(10): 772–780.
- 29 Youssef LA, Rebbaa A, Pampou S, Weisberg SP, Stockwell BR, Hod EA, Spitalnik SL. Increased erythrophagocytosis induces ferroptosis in red pulp macrophages in a mouse model of transfusion. *Blood* 2018; 131(23): 2581–2593.
- 30 Linkermann A, Skouta R, Himmerkus N, Mulay SR, Dewitz C, De Zen F, Prokai A, Zuchtriegel G, Krombach F, Welz PS, Weinlich R, Vanden Berghe T, Vandenabeele P, Pasparakis M, Bleich M, Weinberg JM, Reichel CA, Brasen JH, Kunzendorf U, Anders HJ, Stockwell BR, Green DR, Krautwald S. Synchronized renal tubular cell death involves ferroptosis. *Proc Natl Acad Sci U S A* 2014; 111(47): 16836–16841.
- 31 Matsushita M, Freigang S, Schneider C, Conrad M, Bornkamm GW, Kopf M. T cell lipid peroxidation induces ferroptosis and prevents immunity to infection. *J Exp Med* 2015; 212(4): 555–568.
- 32 Gao M, Monian P, Jiang X. Metabolism and iron signaling in ferroptotic cell death. *Oncotarget* 2015; 6: 1–2.
- 33 Yang WS, SriRamaratnam R, Welsch ME, Shimada K, Skouta R, Viswanathan VS, Cheah JH, Clemons PA, Shamji AF, Clish CB, Brown LM, Girotti AW, Cornish VW, Schreiber SL, Stockwell BR. Regulation of ferroptotic cancer cell death by GPX4. *Cell* 2014; 156(1–2): 317–331.
- 34 Gaschler MM, Stockwell BR. Lipid peroxidation in cell death. *Biochem Biophys Res Commun* 2017; 482(3): 419–425.
- 35 Sun X, Ou Z, Chen R, Niu X, Chen D, Kang R, Tang D. Activation of the p62-Keap1-NRF2 pathway protects against ferroptosis in hepatocellular carcinoma cells. *Hepatology* 2016; 63(1): 173–184.
- 36 Gutteridge JM, Mumby S, Quinlan GJ, Chung KF, Evans

- TW. Pro-oxidant iron is present in human pulmonary epithelial lining fluid: implications for oxidative stress in the lung. *Biochem Biophys Res Commun* 1996; 220(3): 1024–1027.
- 37 Upton RL, Chen Y, Mumby S, Gutteridge JMC, Anning PB, Nicholson AG, Evans TW, Quinlan GJ. Variable tissue expression of transferrin receptors: relevance to acute respiratory distress syndrome. *Eur Respir J* 2003; 22(2): 335–341.
- 38 Wesselius LJ, Nelson ME, Skikne BS. Increased release of ferritin and iron by iron-loaded alveolar macrophages in cigarette smokers. *Am J Respir Crit Care Med* 1994; 150: 690–695.
- 39 Hou W, Xie Y, Song X, Sun X, Lotze MT, Zeh HJ 3rd, Kang R, Tang D. Autophagy promotes ferroptosis by degradation of ferritin. *Autophagy* 2016; 12(8): 1425–1428.
- 40 Wang YQ, Chang SY, Wu Q, Gou YJ, Jia L, Cui YM, Yu P, Shi ZH, Wu WS, Gao G, Chang YZ. The protective role of mitochondrial ferritin on erastin-induced ferroptosis. *Front Aging Neurosci* 2016; 8: 308.